NONLINEAR DYNAMICS OF FIELD DOMAINS IN WEAKLY DISORDERED SUPERLATTICES

F. PRENGEL, M. PATRA, G. SCHWARZ, AND E. SCHÖLL

Institut für Theoretische Physik, Technische Universität Berlin,
Hardenbergstraße 36, 10623 Berlin, Germany

We analyze the bifurcation scenarios and phase diagrams of weakly coupled superlattices and demonstrate how the different regimes are influenced by structural disorder, e.g. doping fluctuations. Furthermore, we show that the dynamics of field domains upon voltage turn-on is governed by the creation and subsequent well-to-well propagation of a charge accumulation layer in the superlattice, which manifests itself by the occurrence of current spikes.

1 Introduction

In weakly coupled semiconductor superlattices, the formation of electric-field domains in the growth direction for sufficient doping or optical excitation, and the occurrence of self-generated current oscillations for lower carrier densities are phenomena well known from both experiments[1] and simulations[2,3,4].

Here we use the simple models presented in Refs. [2,5] for a sample composed of $N = 40$ GaAs quantum wells (n-doped with concentration $N_D^{(i)}$ in the ith well) separated by AlAs barriers. Frozen-in doping fluctuations are modelled by $N_D^{(i)} = N_D(1 + \alpha_i)$, $\alpha_i \in [-\alpha, \alpha]$, where the parameter α characterizes the amount of disorder present in the sample. The electric field is calculated self-consistently from Poisson's law, and contacts are modelled by "virtual" wells with fixed electron densities, thus acting as a carrier reservoir.

2 Bifurcation scenarios

The calculated phase diagram of a superlattice without fluctuations of the heteroparameters as a function of doping density and applied voltage is presented in Fig. 1. One can distinguish several regimes which are associated with characteristic bifurcation scenarios (Figs. 1a-f).

For very low doping, the uniform electric field in the sample results in a two-peak-structure of the current $j(U)$ due to resonant tunneling (Fig. 1a).

At higher doping, spatio-temporal instabilities lead to the build-up of space charges, which results in self-oscillations of the current (Fig. 1c). These limit cycle oscillations are generated by supercritical Hopf bifurcations[6]. They vanish above a certain doping threshold (Fig. 1d).
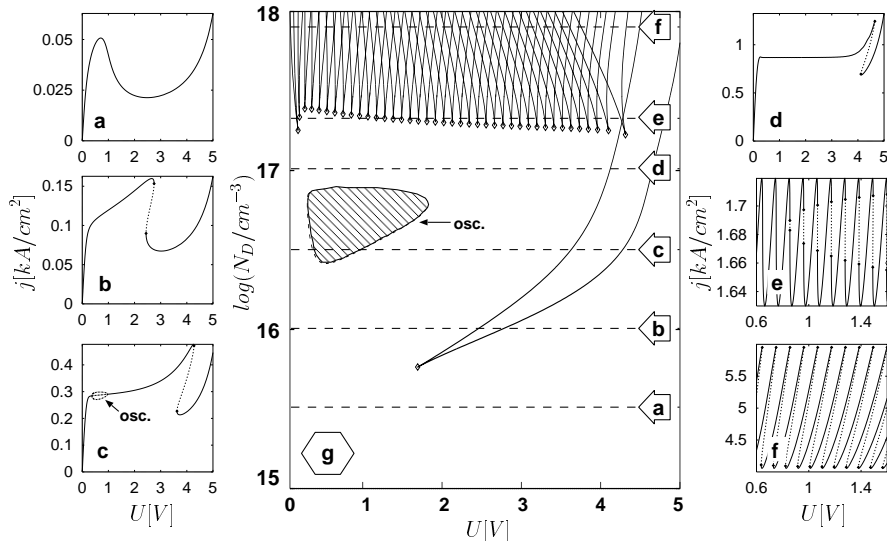
Figure 1: (a-f) Bifurcation scenarios of a superlattice without disorder for different doping densities. Solid (dotted) lines correspond to stable (unstable) steady states. (g) Corresponding phase diagram as a function of doping N_D and applied voltage U. (solid lines – saddle-node bifurcations, shaded region – oscillations, $\diamond$ – cusp points)

At the highest doping densities (1e,f), the available carrier density is sufficient to provide the space charge for the formation of a stable boundary between a low-field and a high-field domain. In this regime, the current-voltage characteristic consists of branches, whose stability is changed from stable to unstable and vice versa by saddle-node bifurcations. Fig. 1g shows the locations of the saddle-node bifurcations as solid lines; they originate from cusp points marked by diamonds ($\diamond$). Two bifurcation scenarios from this regime are shown in Figs. 1e and 1f. While unstable branches only start to develop in Fig. 1e, they are fully present in Fig. 1f, indicating the formation of field domains with a well-defined boundary in between.

The influence of doping fluctuations on the phase diagram and current-voltage characteristic is demonstrated in Fig. 2 for the disorder parameter $\alpha = 8\%$. The locations of both the Hopf and saddle-node bifurcations are influenced. This has considerable impact on the static current-voltage characteristic under domain formation; it may even lead to the disappearance of current branches in the measured characteristics [7]. The amplitude and frequency of the current self-oscillations, however, are only slightly influenced [6].
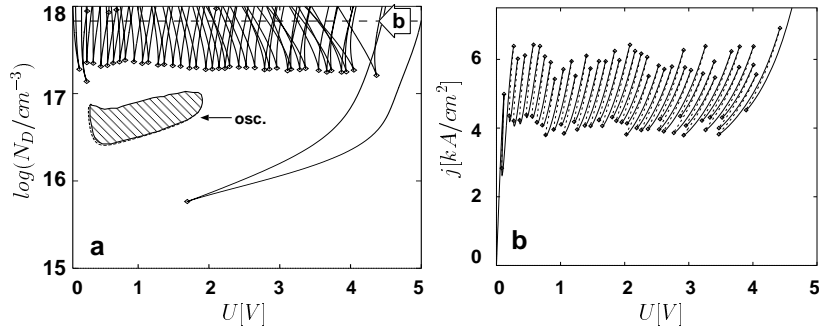
Figure 2: (a) Phase diagram and (b) bifurcation scenario of a highly doped superlattice with $\alpha = 8\%$ doping disorder.

3   Domain dynamics

In this section, we demonstrate how the sequential tunneling in weakly coupled superlattices manifests itself in the time dependence of the current density, both for domain formation and self-oscillations.
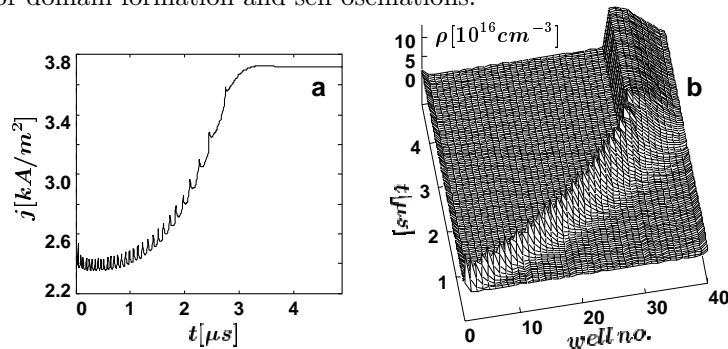

Figure 3: (a) Current response and (b) spatial charge distribution of a superlattice ($N_D = 1.67 \cdot 10^{17} cm^{-3}$) for an applied voltage step of $1V$.

Fig. 3 shows the current response (a) and spatial charge distribution (divided by $-e$) as a function of time (b) of a highly doped ($N_D = 1.67 \cdot 10^{17} cm^{-3}$) superlattice (with $\alpha = 2\%$), calculated with the model of Ref. [4], when the applied voltage is instantaneously switched on from 0 to $1V$. As can be seen from Fig. 3b, a charge accumulation layer forms at the cathode (well no. 0) immediately after the voltage is turned on and propagates towards the anode hopping from well to well until it reaches a stable position, thus forming the boundary between a high-field and a low-field domain. The hopping of the accumulation layer from well to well is accompanied by a sequence of small
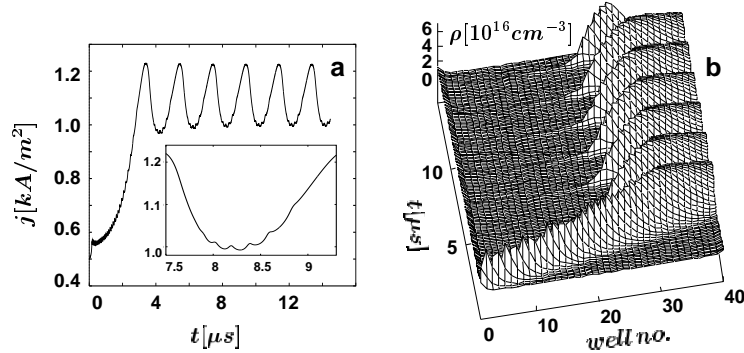
3

current spikes in Fig. 3a (seen also in experiments[5]).

Figure 4: (a) Current response and (b) spatial charge distribution of a superlattice ($N_D = 3.34 \cdot 10^{16} cm^{-3}$) for an applied voltage step of $1V$. The inset in (a) shows an enlarged section of one current oscillation.

This very same phenomenon is found in the regime of lower doping, where current self-oscillations occur. In Fig. 4 we show the current density (a) and spatial charge distribution (b) for $N_D = 3.34 \cdot 10^{16} cm^{-3}$. The same voltage step of $1V$ is applied at time $t = 0$, and the same slow initial rise of the current, accompanied by small current spikes, can be observed. However, no stable domains are eventually formed. Instead, an oscillatory instability gives rise to self-oscillations with small superimposed current spikes indicating that also in this regime transport is dominated by well-to-well hopping of the space charge.

References

1. J. Kastrup *et al.*, *Phys. Rev.* B **52**, 13761 (1995).
2. F. Prengel, A. Wacker, and E. Schöll, *Phys. Rev.* B **50**, 1705 (1994).
3. L. L. Bonilla *et al.*, *Phys. Rev.* B **50**, 8644 (1994).
4. A. Wacker, F. Prengel, and E. Schöll in *Proc. 22nd ICPS*, ed. D. J. Lockwood (World Scientific, Singapore, 1995), p. 1075.
5. J. Kastrup, F. Prengel, H. T. Grahn, K. Ploog, and E. Schöll, *Phys. Rev.* B **53**, 1502 (1996).
6. M. Patra, Diplomarbeit, Technische Universität Berlin (1996).
7. G. Schwarz *et al.*, *Semicond. Sci. Technol.* **11**, 475 (1996).